Downloaded By: [ETH Eidgenoessische Technische Hochschule] At: 11:49 13 January 200

Ferroelectrics, 359:14–20, 2007
Copyright © Taylor & Francis Group, LLC
ISSN: 0015-0193 print / 1563-5112 online
DOI: 10.1080/00150190701512185

Taylor & Francis
Taylor & Francis Group

Ferroelectric Domains in Thin Films and Superlattices: Results of Numerical Modeling

F. DE GUERVILLE,[1] M. EL MARSSI,[1] I. LUKYANCHUK,[1,*] AND L. LAHOCHE[2]

[1]Condensed Matter Physics Laboratory, University of Picardie, Amiens, France
[2]Roberval Laboratory, University of Technology of Compiegne, France

In micro- and nanoscale ferroelectric samples, a formation of periodic polarization domains is the efficient mechanism of reducing depolarization field that is produced by the surface bound charges. This makes the physics of these samples different from the bulk samples. We present the results of modelling of ferroelectric domains and domain textures in ferroelectric thin films and periodic paraelectric/ferroelectric superlattices, basing on the self-consistent solution of the coupled electrostatic and Ginzburg-Landau equations. We go beyond the traditionally used low-temperature Kittel approximation (in which the polarization is assumed to be temperature independent and constant across domains) and explore the temperature evolution of the domain-induced properties. For numerical solution of the problem, we use the finite-element PDE tool-box that allows to work over the entire temperature interval and in a wide region of sample parameters.

Keywords Ferroelectric domain; thin film; superlattice; modelling

PACS numbers: 77.55.+f, 77.80.Dj, 77.80.Bh

I. Introduction

In recent years, a lot of attention was given to studies of finite size, surface and interface effects in ferroelectric thin films and superlattices [1] because of their potential applications as units of Ferroelectric Random Access Memory. Such devices have the most interesting ferroelectric properties as the polarization is oriented in a perpendicular to the film surface c-direction. It is well-known, however, that the surface discontinuity of polarization induces the bounded charges ρ (r) = div **P** that produce the internal depolarizing electric field. To diminish the associated electrostatic energy $F_{dep} \sim E^2/4\pi$ the sample is divided into ferroelectric domains with alternated "up" and "down" polarization. The energy F_{dep} in this case becomes smaller since depolarization field concentrates closer to the film surface and does not penetrate into the volume, but a new contribution due to domain wall energy $F_{dw} \sim (a_f/d)P^2$ appears.

A delicate balance between depolarization F_{dep} and domain wall F_{dw} energies provides the equilibrium domain configuration. The domain formation in the bulk ferroelectric samples [2–5] and in thin films [6,7] was studied in so-called Kittel approximation [2] in which the polarization profile across domains is supposed to be flat and temperature independent,

Received October 26, 2006; in final form January 17, 2007.
*Corresponding author. E-mail: lukyanc@ferroix.net

Downloaded By: [ETH Eidgenoessische Technische Hochschule] At: 11:49 13 January 200

and domain walls are infinitively thin. Being justified at low temperatures this approach is not valid close to ferroelectric-paraelectric transition temperature T_c where the polarization gradient is very soft because of the divergence of the coherence length [8]. In the present work we perform the modelling of domain structure in a whole temperature interval and study the temperature evolution of the related properties of the film.

1. Model Description

The studied configuration of ferroelectric film with 180° periodic domain texture that is sandwiched between two paraelectric layers and placed into the short-circuited capacitor is analogous to the problem of ferroelectric/paraelectric superlattice with periodic (along c) boundary conditions, as shown in Figure 1a. The space distribution of ferroelectric

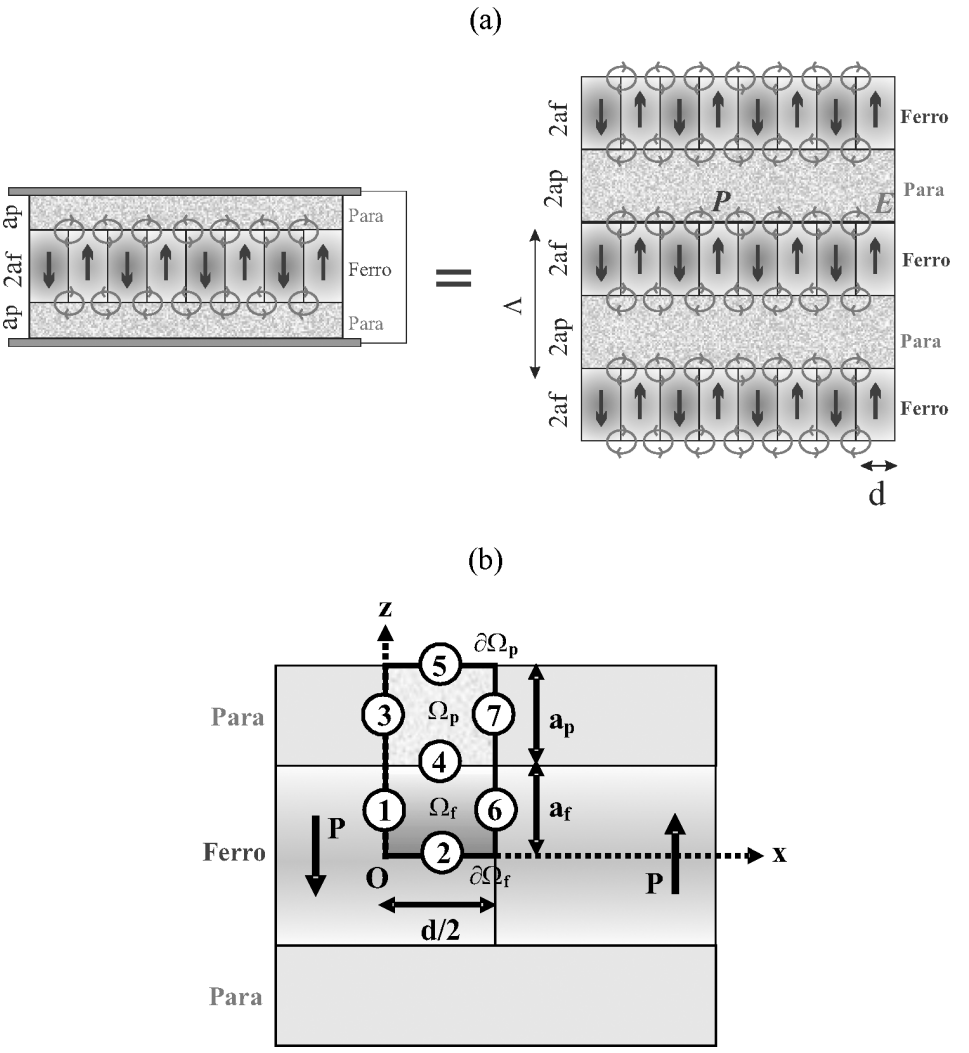

Figure 1. (a) Capacitor-like and superlattice-like geometry of the problem. (b) Elementary region used for the modelling. (See Color Plate VI)

Downloaded By: [ETH Eidgenoessische Technische Hochschule] At: 11:49 13 January 200

polarization P(x,z) and electrostatic potential φ(x,z) are described by the coupled electrostatic and dimensionless nonlinear Ginzburg-Landau equations [8,9]:

$$\mathrm{div}(\mathbf{E} + 4\pi\mathbf{P}) = 0,\ \mathrm{rot}\ \mathbf{E} = 0, \tag{1}$$

$$-\nabla^2 \mathrm{P} + (\mathrm{t} + \mathrm{P}^2)\mathrm{P} = \frac{\varepsilon_{//}}{4\pi} E_z^{(\mathrm{f})}, \tag{2}$$

where the reduced temperature t is expressed via the bulk critical temperature T_{c0} as $t = T/T_{c0} - 1$, the dimensionless parameter $\varepsilon_{//} \gg 1$ is expressed via the Curie constant: $\varepsilon_{//} = C/T_{c0}$, the spontaneous z-compound of ferroelectric polarization $P = P_z^{(f)}$ is measured in units of the bulk polarization P_0 at $T = 0$ and all the space coordinates are scaled in units of zero-temperature coherence length ξ_0. The induced x-component of polarization $P_x^{(f)}$ as well as the polarization in paraelectric layer is linearly related to corresponded electric fields:

$$\mathrm{P}_{\mathrm{x}}^{(\mathrm{f})} = \frac{\varepsilon_{\perp} - 1}{4\pi}\mathrm{E}_{\mathrm{x}}^{(\mathrm{f})}, \quad \mathrm{P}_{\mathrm{x,z}}^{(\mathrm{p})} = \frac{\varepsilon_{\mathrm{p}} - 1}{4\pi}\mathrm{E}_{\mathrm{x,z}}^{(\mathrm{p})} \tag{3}$$

The conventional electrostatic boundary conditions at the para/ferro interface:

$$E_{\mathrm{z}}^{(\mathrm{f})} - E_{\mathrm{z}}^{(\mathrm{p})} = -4\pi\left(P_{\mathrm{z}}^{(\mathrm{f})} - P_{\mathrm{z}}^{(\mathrm{p})}\right), \quad E_{\mathrm{x}}^{(\mathrm{f})} = E_{\mathrm{x}}^{(\mathrm{p})} \tag{4}$$

are completed by boundary condition [10] for spontaneous ferroelectric polarization

$$\partial_{\mathrm{z}}\mathrm{P} = \lambda\mathrm{P}, \tag{5}$$

where λ is the extrapolation length (we assumed that $\lambda = 0$).

II. Model Implementation

For numerical modelling we used the nonlinear iterative Newton-Raphson algorithm realized in the Comsol Multiphysics Finite-Element toolbox [11]. The symmetry of the periodic domain structure let us to perform the calculations in the elementary region presented in Figure 1b. This region of the half domain width d/2 is composed from the paraelectric subregion Ω_p with boundary $\partial\Omega_p = (2) + (3) + (4) + (7)$ and height a_p and ferroelectric subregion Ω_f with boundary $\partial\Omega_f = (1) + (2) + (4) + (6)$ and height a_f.

It was convenient to map the elementary region Ω_f onto the unit square cell, using the coordinate rescaling $\tilde{x} = 2x/d$ and $\tilde{z} = z/a_f$ where $0 \le \tilde{x} \le 1$ and $0 \le \tilde{z} \le 1$ and using the scalar electrostatic potential φ instead of the vector electrical field $\mathbf{E} = -\nabla\varphi$. Finally, we got the system of partial nonlinear differential equations (PDE) with three independent variables: $u = (P, \varphi, \varphi')$ that can be formalized as:

$$\mathrm{d_a}\frac{\partial \mathrm{u}}{\partial \mathrm{t}} + \nabla.(-\mathrm{c}\nabla\mathrm{u} - \alpha\mathrm{u} + \gamma) + \beta.\nabla\mathrm{u} + \mathrm{au} = \mathrm{f}, \tag{6}$$

where coefficients are given by the following relations:

For P in Ω_f:

$$\mathrm{d_a} = 0, \quad \mathrm{c} = \left\langle \frac{4}{\mathrm{d}^2} \quad \frac{1}{\mathrm{a_f^2}} \right\rangle, \quad \alpha = \beta = \gamma = 0, \quad \mathrm{a} = \mathrm{t} + \mathrm{P}^2, \quad \mathrm{f} = -\frac{\varepsilon_{//}}{4\pi\,\mathrm{a_f}}\frac{\partial\varphi}{\partial\tilde{\mathrm{z}}}$$

Downloaded By: [ETH Eidgenoessische Technische Hochschule] At: 11:49 13 January 200

For φ in Ω_f:

$$d_a = 0, \quad c = \left\langle \frac{4\varepsilon_\perp}{d^2} \quad \frac{1}{a_f^2} \right\rangle, \quad \alpha = \beta = \gamma = 0, \quad a = 0, \quad f = -\frac{4\pi}{a_f}\frac{\partial P}{\partial \tilde{z}}$$

For φ' in Ω_p:

$$d_a = 0, \quad c = \left\langle \frac{4}{d^2} \quad \frac{1}{a_f^2} \right\rangle, \quad \alpha = \beta = \gamma = 0, \quad a = 0, \quad f = 0$$

The corresponding boundary conditions:

$$P = 0, \varphi = 0. \tag{BC1}$$

$$\frac{\partial P}{\partial \tilde{z}} = 0, \quad \varphi = 0. \tag{BC2}$$

$$\varphi' = 0. \tag{BC3}$$

$$\frac{\partial P}{\partial \tilde{z}} = a_f \lambda P = 0, \quad \varphi = \varphi', \quad \frac{\partial \varphi}{\partial \tilde{z}} - \varepsilon_p \frac{\partial \varphi'}{\partial \tilde{z}} = 4\pi a_f P. \tag{BC4}$$

$$\varphi' = 0. \tag{BC5}$$

$$\frac{\partial P}{\partial \tilde{x}} = 0, \quad \frac{\partial \varphi}{\partial \tilde{z}} = 0. \tag{BC6}$$

$$\frac{\partial \varphi'}{\partial \tilde{x}} = 0. \tag{BC7}$$

are written either in Neumann:

$$n.(c\nabla u + \alpha u - \gamma) + qu = g - h^T \mu, \tag{7}$$

or in Dirichlet form:

$$hu = r, \tag{8}$$

where coefficients are given in the Table I.

We have used the realistic values of material parameters $\varepsilon_{//} = 500$, $\varepsilon_\perp = 100$, $\varepsilon_p = 10$ and $\xi_0 \approx 1$ nm. The width of the paraelectric layer $2a_f$ was selected between 25 and 1000 nm whereas a_p was always larger than a_f to ensure the multi-domain structure of the sample.

Table 1
Coefficients for the boundary conditions (7) and (8)

Boundary	(1)		(2)		(3)		(4)		(5)	(6)	(7)	
Variable	P	φ	P	φ	φ'	P	φ	φ'	φ'	P	φ	φ'
q	0	0	0	0	0	0	0	0	0	0	0	
g	0	0	0	0	0	0	$4\pi P a_f + \varepsilon_p \frac{\partial \varphi'}{\partial \tilde{z}}$	0	0	0	0	0
h	1	1	—	1	1	—	0	1	1	—	—	—
r	0	0	—	0	0	—	0	φ	0	—	—	—

Downloaded By: [ETH Eidgenoessische Technische Hochschule] At: 11:49 13 January 200

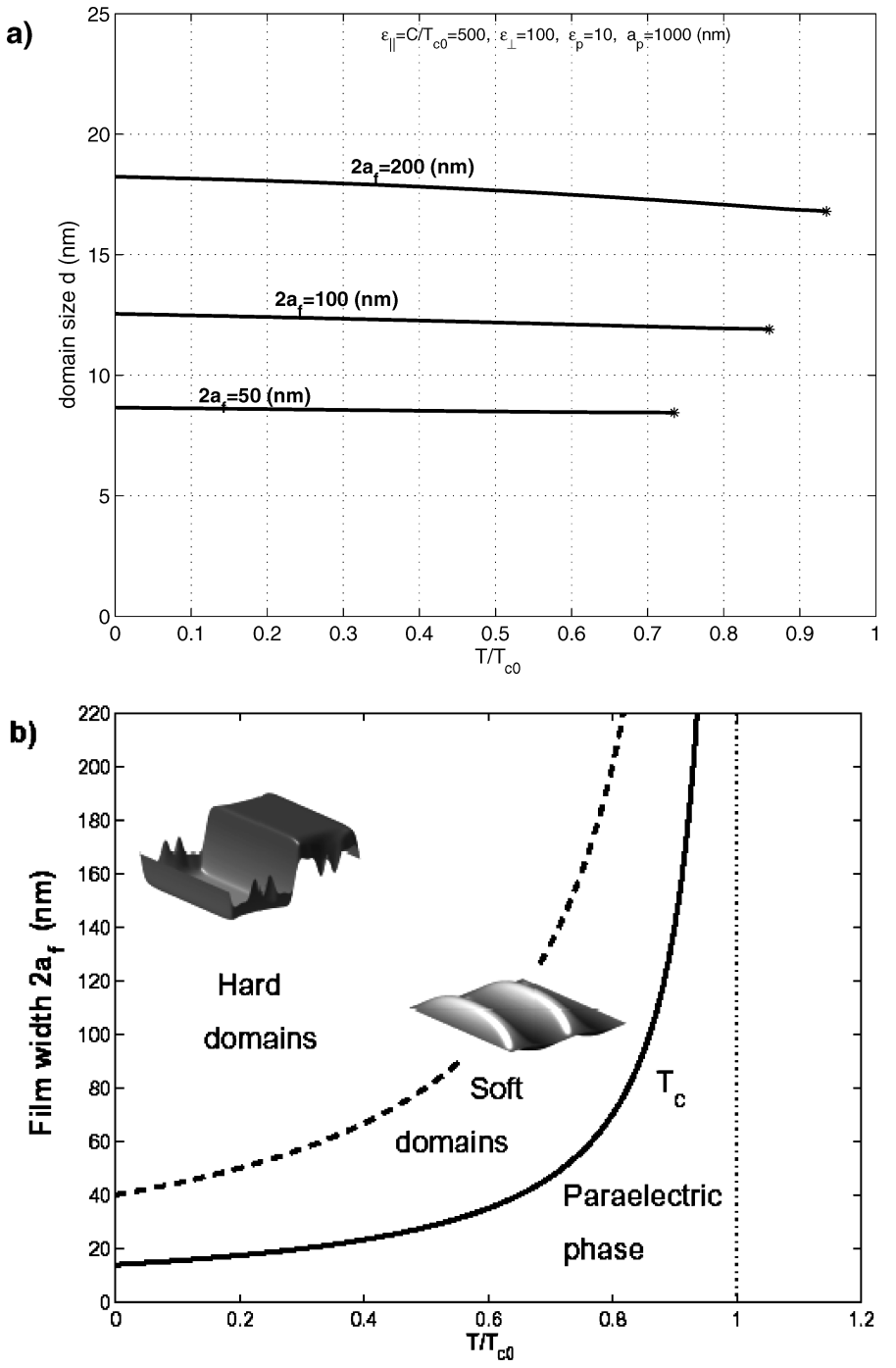

Figure 2. (a) Dependence of domain size on the temperature for the films with different width. (b) Phase diagram of the ferroelectric film with domain structure. Solid line presents the transition from the paraelectric to multidomain ferroelectric phase. Dashed line presents the crossover from soft- to hard-domain state. The corresponding hard- and soft-polarization profiles P(x,z) inside domains are shown. (See Color Plate VII)

Downloaded By: [ETH Eidgenoessische Technische Hochschule] At: 11:49 13 January 200

The developed code allowed us to calculate the distribution of polarization inside domain P(x,z). Among the domain textures with different periods 2d, we selected those that minimize the Landau free energy

$$F = -\frac{1}{4}\int_{\Omega} P^4 dxdz \tag{9}$$

Such a way we got the evolution of the domain size as function of temperature for the different film width presented in Figure 2a.

III. Results

The principal results of the modelling are presented in Figure 2. Calculating the polarization profile P(x,z) inside the stable domain structure, we checked that the Kittel approximation of "hard" domain structure [2,3,6] is well satisfied at low temperatures. At the same time, close to T_c domains have the "soft" sinus-like profile, as was predicted by linearized Ginzburg-Landau theory [8,9]. The resulting phase diagram is presented in Figure 2b.

The "hard" domains are realized mostly in thick films and in the low temperature region whereas the "soft" domains should exist in thin films and at higher temperatures. We can predict therefore that the domain-provided ferroelectric properties of thin and thick films (such as thermodynamics, frequency dispersion of susceptibility, hysteresis of polarization, domain wall pinning etc.) should be different because of the different domain profile structures. We obtained also that the critical temperature of transition into the ferroelectric phase with domains is strongly suppressed as the film widths vanishes (see Figure 2b). In contrast, we found that the presented in Figure 2a temperature dependence of the domain size is very week.

Acknowledgment

This work was supported by region of Picardie, France.

References

1. M. Dawber, K. M. Rabe, and J. F. Scott, Physics of thin-film ferroelectric oxides. *Rev. Mod. Phys.* **77**, 2005 and references therein.
2. C. Kittel, Theory of the Structure of Ferromagnetic Domains in Films and Small Particles. *Phys. Rev.* **70**, 965 (1946).
3. L. D. Landau and E. M. Lifshitz, Electrodynamics of Continuous Media. New York: Elsevier; 1985.
4. C. L. Wang, Surface effect on ferroelectric domain structure. *Solid State Commun.* **82**, 743 (1992).
5. B. M. Darinskii, A. P. Lazarev, and A. S. Sidorkin, Formation of the domain-structure by the cooling of ferroelectric surface. *Ferroelectrics*. **98**, 241 (1989).
6. A. M. Bratkovsky and A. P. Levanuk, Abrupt Appearance of the Domain Pattern and Fatigue of Thin Ferroelectric Films. *Phys. Rev. Lett*. **84**, 3177 (2000); A. M. Bratkovsky and A. P. Levanuk, Very large dielectric response of thin ferroelectric films with the dead layers. *Phys. Rev.* **B63**, 132103 (2001).
7. P. Mokry, A. K. Tagantsev, and N. Setter, Size effect on permittivity in ferroelectric polydomain thin films. *Phys. Rev.* **B70**, 172107 (2004).

Downloaded By: [ETH Eidgenoessische Technische Hochschule] At: 11:49 13 January 200

8. E. V. Chensky and V. V. Tarasenko, Theory of phase-transitions to inhomogeneous states in finite ferroelectrics in an external electric-field. *Sov. Phys. JETP.* **56**, 618 (1982) [Zh. Eksp. Teor. Fiz. **83**, 1089 (1982)].
9. V. A. Stephanovich, I. A. Luk'yanchuk, and M. G. Karkut, Domain-Enhanced Interlayer Coupling in Ferroelectric/Paraelectric Superlattices. *Phys. Rev. Lett.* **94**, 047601 (2005).
10. R. Kretschmer and K. Binder, Surface effects on phase transitions in ferroelectrics and dipolar magnets. *Phys. Rev.* **B20**, 1065 (1979).